Original article
EDN: ERLVOT
DOI: 10.21285/2686-9993-2026-49-1-8

Comparative assessment of satellite and unmanned aerial vehicles data for landslide susceptibility mapping

Svetlana A. Gantimurova[a], Alexander V. Parshin[b]✉, Guanwen Huang[c] Junyuan Li[d], Ce Jing[e], Vyacheslav T. Zalutskii[f]

[a,b,f]*Irkutsk National Research Technical University, Irkutsk, Russian Federation*
[b]*A.P. Vinogradov Institute of Geochemistry, Siberian Branch of the Russian Academy of Sciences, Irkutsk, Russian Federation*
[c–e]*Chang'an University, Xi'an, China*

Abstract. Remote sensing methods enable the rapid study of large, hard-to-reach areas prone to hazardous gravitational geological processes (landslides, rockfalls). Regional mapping of high-risk landslide areas based on satellite remote sensing data is already well-developed. In recent decades, the theory and practice of using unmanned aerial vehicle (UAV) technologies for remote sensing have rapidly evolved. In both cases, multispectral survey data and digital elevation models are used to analyze geological risks. The purpose of the presented research is to compare the results of landslide susceptibility mapping based on available satellite data and unmanned aerial vehicles data and to identify the advantages and limitations of both methods. The key predictors for satellite data (slope angles, profile curvature, normalized difference vegetation index, wetness index and length-slope factor) were derived from ALOS AW3D30 digital evaluation models and Sentinel-2 data. Unmanned aerial vehicle data were obtained using a photogrammetric method with multispectral cameras. To determine the weights of factors, the analytical hierarchy process was used through pairwise comparisons. Landslide susceptibility maps were generated for the same area using QGIS. The comparative analysis has clearly demonstrated how differences in input data resolution and survey methodology impact the predictive value of the results. The major finding is that due to resolution generalization (in the case of satellite imagery) small, unstable rock blocks can artificially increase the vulnerability of adjacent slopes, on the other hand, some small, but hazardous rocks can remain completely unnoticed. At the same time, it is shown that high-resolution data from unmanned aerial vehicles do not replace satellite remote sensing data, but rather complement it. The methods serve different spatial scales and research objectives. The results confirm that satellite data and data from unmanned aerial vehicles should be complementary. Satellite data are suitable for regional landslide susceptibility mapping, while data from unmanned aerial vehicles are essential for detailed studies of individual areas identified using satellite data. Therefore, a hybrid methodology is recommended: satellite data for the initial zoning of hazardous areas, and data from unmanned aerial vehicles for the detailed study of hazardous areas.

Keywords: landslide susceptibility mapping, satellite remote sensing, unmanned aerial vehicle, remote sensing

For citation: Gantimurova S.A., Parshin A.V., Huang G., Li J., Jing C., Zalutskii V.T. Comparative assessment of satellite and unmanned aerial vehicles data for landslide susceptibility mapping. *Earth sciences and subsoil use*. 2026;49(1):96-110. https://doi.org/10.21285/2686-9993-2026-49-1-8.

Научная статья
УДК 624.131.31

Сравнительная оценка информативности спутниковых данных и данных с беспилотных летательных аппаратов при решении задач картирования оползневой опасности

С.А. Гантимурова[a], А.В. Паршин[b]✉, Г. Хуан[c], Ц. Ли[d], Ц. Цзин[e], В.Т. Залуцкий[f]

[a,b,f]Иркутский национальный исследовательский технический университет, Иркутск, Российская Федерация
[b]Институт геохимии им. А.П. Виноградова Сибирского отделения Российской академии наук, Иркутск, Российская Федерация
[c–e]Чанъаньский университет, Сиань, Китай

Резюме. Использование методов дистанционного зондирования Земли позволяет быстро изучать большие по площади и труднодоступные территории, в пределах которых могут происходить опасные гравитационные геологические процессы (оползни, камнепады). Картирование оползневых зон на основе спутниковых данных в региональном масштабе на сегодняшний день уже хорошо развито на практике. В последние десятилетия стремительно развиваются теория и практика применения технологий беспилотных летательных аппаратов для дистанционного зондирования Земли. В обоих случаях для анализа георисков используются мультиспектральные данные и цифровые модели рельефа. Целью данного исследования является сравнительный анализ результатов картирования оползневой опасности, полученных на основе общедоступных спутниковых данных и данных с беспилотных летательных аппаратов, и выявление преимуществ и ограничений обеих методик. Ключевые предикторы (углы уклона склонов, профильная кривизна, нормализованный относительный индекс растительности, индекс влажности и коэффициент длины-уклона) для спутниковых данных были получены из цифровых моделей рельефа ALOS AW3D30 и данных Sentinel-2. Данные с беспилотных летательных аппаратов были получены фотограмметрическим методом с помощью мультиспектральных фотокамер. Для определения весов факторов применялся метод аналитической иерархии через попарные сравнения. Средствами QGIS построены карты рисков оползневых процессов для одного и того же участка территории. Сравнительный анализ наглядно показал, как различие в разрешении входных данных и методике съемок влияет на прогностическую ценность результатов. Основной вывод: из-за генерализации по разрешению (в случае спутниковых съемок) небольшие неустойчивые скальные блоки могут либо искусственно увеличивать уязвимость прилегающих склонов, либо оставаться полностью незамеченными. В то же время показано, что данные высокого разрешения с беспилотных летательных аппаратов не заменяют данные спутниковых дистанционных зондирований Земли, а дополняют их, методы служат разным пространственным масштабам работ и исследовательским задачам. Результаты подтверждают, что спутниковые данные и данные с беспилотных летательных аппаратов должны быть комплементарны. Спутниковые данные подходят для регионального картирования модели поверхности земли (Landslide Susceptibility Mapping), а данные с беспилотных летательных аппаратов необходимы для детальных исследований отдельных участков, выделенных по спутниковым данным. Рекомендуется гибридная методология: космические данные – для первичного зонирования опасных зон, а беспилотные летательные аппараты – для детального изучения опасных участков.

Ключевые слова: картирование оползневой опасности, спутниковое дистанционное зондирование Земли, беспилотный летательный аппарат, дистанционное зондирование Земли

Для цитирования: Гантимурова С.А., Паршин А.В., Хуан Г., Ли Ц., Цзин Ц., Залуцкий В.Т. Сравнительная оценка информативности спутниковых данных и данных с беспилотных летательных аппаратов при решении задач картирования оползневой опасности // Науки о Земле и недропользование. 2026. Т. 49. № 1. С. 96–110. https://doi.org/10.21285/2686-9993-2026-49-1-8.

Introduction

Landslides are exogenous geological processes that pose a serious danger to infrastructure and human health. Rockfalls, scree and landslides occurring in populated and built-up areas can lead to considerable financial damage. Inventory and mapping of landslides on different scales is an important direction of fundamental and applied research. Landslide susceptibility mapping (LSM) is a valuable technique for delineation of landslide-prone areas, which is based on a factor analysis considering

the contribution of topographic, geological, hydrological and land cover conditions [1, 2]. The output maps allow development of proactive mitigation strategies to prevent or minimize economic losses and threats to human life.

The primary data sources for LSM include landslide inventory data, conditioning factor data (environmental and topographic variables), and triggering factor data (precipitation, seismic activity etc.). These data can be obtained through field surveys, existing geospatial databases or remote sensing.

Traditional landslide susceptibility mapping relies primarily on direct observation and manual interpretation of terrain features. Field mapping involves direct examination of landslide morphology, lithology, and structural discontinuities, providing high accuracy at a local scale but limited spatial coverage, especially in hard-to-reach areas [3].

The use of remote sensing methods to detect unstable slopes has several advantages over field surveys [3–5]. Satellite data for LSM are widely used. It has a great coverage, multitemporal images and data up to 10 m resolution are free-access and covered globally. Sentinel-2 multispectral imagery is utilized in numerous scientific studies [6–9]. Global digital elevation models (DEMs) are in high demand as a product for research in geomorphology and geology due to its availability. Among the most frequently used spaceborne DEMs are ASTER and SRTM [10]. Although landform changes occur slowly, studying exogenous geological processes, which can happen rapidly, requires up-to-date data. AW3D30 data set is a global DEM with a horizontal resolution of 30 metres. It is provided by the Panchromatic Remote-Sensing Instrument for Stereo Mapping (PRISM), an optical sensor aboard the Advanced Land Observing Satellite (ALOS), which is available for use free of charge [10, 11]. Issues with timely data acquisition and interference from atmospheric conditions are some limitations of spaceborne data [12].

Multispectral and radar satellite remote sensing data are often used to study hazardous slope gravity processes at the regional level, since the advantage of satellite data is the accessibility of any territory. However, low-resolution maps can underestimate the risk in potentially unstable areas. Therefore, more sophisticated predictive modelling and validation tools are needed to improve the reliability of maps and minimize future impacts. There is plenty of commercially available high-resolution satellite imagery that provides the necessary spatial detail. Although, significant problem with using high-resolution commercial satellite imagery (0.3–0.5 m) is the so-called “overhead of unnecessary territory”. Such data is distributed not as individual points, but in minimal scenes – for example, 25 or even 100 km². As a result, if the zone of interest is a linear feature (such as a landslide slope or a slide furrow) measuring only 0.5 km², payment is still required for the entire scene, regardless of the actual area of interest. This results in the cost of useful data being artificially inflated by 50–200 times compared to the actual survey area [13]. This creates a significant disadvantage over UAV surveys, where the operator incurs costs only for a precisely defined area of interest.

In recent years, the rapid development of low-cost and small-sized unmanned aerial vehicles (UAV), coupled with improvements in the cost and size of traditional sensors, has led to the emergence of innovative and promising areas in the field of environmental remote sensing, surface modelling and monitoring [4]. Remote sensing using UAVs offers several advantages, including real-time application, flexible survey planning, high resolution, and the capability to gather information in hazardous conditions without posing a risk to the environment [5]. UAVs are effective for conducting detailed studies of small areas, but unsuitable for regional mapping. However, for linear objects such as pipelines, roads or coastal lines, UAVs can be an a highly suitable and effective tool for monitoring and inspection.

Both sources of land surface data have a number of advantages and limitations. The choice depends on many factors and research objectives. Although many studies address data quality and intercomparisons of space-based systems (e.g., ASTER, SRTM, ALOS AW3D30), the overwhelming majority focus on medium- or

high-resolution satellite imagery [10, 11]. Far less attention has been paid to comparing satellite data with high-resolution UAV data, and studies that do so within a single methodological pipeline for landslide susceptibility mapping remain exceptionally rare.

Given research aimed to compare the use of accessible low-resolution satellite data and high-resolution UAV data for LSM, explore the advantages and limitations in a specific case, examine practical applicability. Landslides as a geological hazard: need for accurate susceptibility maps.

Materials and methods

Study area. The Circum-Baikal Railway is located in the Irkutsk region of Russia; its construction began in the late 19th century. Currently, it is used primarily for tourism. The railway tracks are located on a bluff surrounded on one side by the shoreline of Lake Baikal and on the other by steep cliffs reaching an angle of 80 degrees. During the construction of the Circum-Baikal Railway, blasting operations were used, which disrupted the natural terrain and increased the likelihood of rock slides and avalanches.

The Baikal region is characterized by complex engineering and geological conditions. The Irkutsk block of the Sharyzhalgay indentation of the Siberian Platform is located along the shores of Lake Baikal, on an 80-kilometer section of the Circum-Baikal Railway. It is composed of metamorphosed igneous and sedimentary rocks: gneisses, metabasites, schists, marbles, and quartzites. The degree of metamorphism varies from amphibolite to granulite facies. The age of Archean rocks is 3.9–2.9 billion years, and that of Paleoproterozoic rocks is 3.1–2.4 billion years. The region is characterized by the polycyclic development of endogenous processes. The Baikal region is located in the permafrost zone (the frozen ground thickness on the coast is up to 10 meters). The relief is erosional and denudational, with narrow valleys and gorges, and the coast is structurally abrasive. Dangerous geomorphological processes are actively developing here: linear erosion and gravitational slope phenomena.

The climate is temperate, sharply continental: winters are cold and long (6–7 months, with an average January temperature of -25…-30°C, and an absolute minimum of -61°C), while summers are warm but short (15 to 20°C). The transitional seasons are short. Spring and early summer are dry, with most precipitation falling in the second half of summer (2–3 times more in summer than in winter). There are many sunny days. Snow cover by early March does not exceed 20 cm, with more than 50 cm on leeward slopes.

Soils are varied: permafrost-taiga and mountain podzolic soils predominate, while rocky alpine tundra soils are found in the upper mountains. Vegetation consists primarily of coniferous and small-leaved forests (larch, pine, cedar, spruce, fir, and birch).

Mapping of modern landslide processes in the study area was conducted primarily at a small scale. A map of hazardous landslide processes was created at a scale of 1:200,000, based on topographic and geological maps, as well as interpretation of 30-meter-resolution Landsat images [14]. This level of mapping detail may be sufficient for regional planning purposes. However, to study small hazardous areas and accurately map the spatial distribution of landslides, larger-scale studies are necessary.

Satellite data. The research utilized up-to-date spaceborne data, which were available at no cost. Morphometric data for region of interest were obtained from the AW3D30 (DEM) with a resolution of 30 m, generated from stereo imagery collected by the Panchromatic Remote-Sensing Instrument for Stereo Mapping (PRISM) aboard the Advanced Land Observing Satellite (ALOS) (Fig. 1). Additionally, 10 m resolution Sentinel-2 imagery, encompassing red, blue, green, and near-infrared bands, was employed for the calculation of spectral indices and for the visual interpretation of the study area (Fig. 2).

Unmanned aerial vehicle data. To obtain the geospatial data necessary for creating a DEM and calculating parameters related to the risk of landslides, a hexacopter with a mounted multispectral camera MAPPIR2 was used. The shooting was carried out at a height of 125 m above the ground, shooting from two camera an-

gles of 45 and 90 (nadir) degrees. The resulting images have the resolution of 10 cm per pixel. The survey followed a network of parallel routes, achieving a longitudinal overlap of 70–80% and a transverse overlap of 60–70% between frames. This approach facilitates the 3D reconstruction of the terrain using image-matching algorithms. After the initial processing of the UAV survey data, photogrammetric processing of the obtained images was carried out using the Structure from Motion algorithm. The obtained results include: DEM (Fig. 3), orthomosaic (Fig. 4), point cloud, textured model (Fig. 5).

Methods. Landslide Susceptibility Mapping (LSM) using the Analytical Hierarchy Process (AHP) became a popular and reliable GIS-based, multi-criteria decision-making method used to identify areas vulnerable to landslides [3, 15–18]. AHP methos determines relative weights for causative factors through pairwise comparisons. Typical variables for LSM models are elevation, slope angle, aspect, curvature, lithology, distance to roads, distance to rivers, and land use/land cover [19]. In order to implement LSM five conditioning factors were derived from spaceborne and UAV data in QGIS (Fig. 6, 7):

1. Slope angle is directly influences gravitational shear stress, runoff velocity, and soil/rock stability [17]. The occurrence of rockfalls and

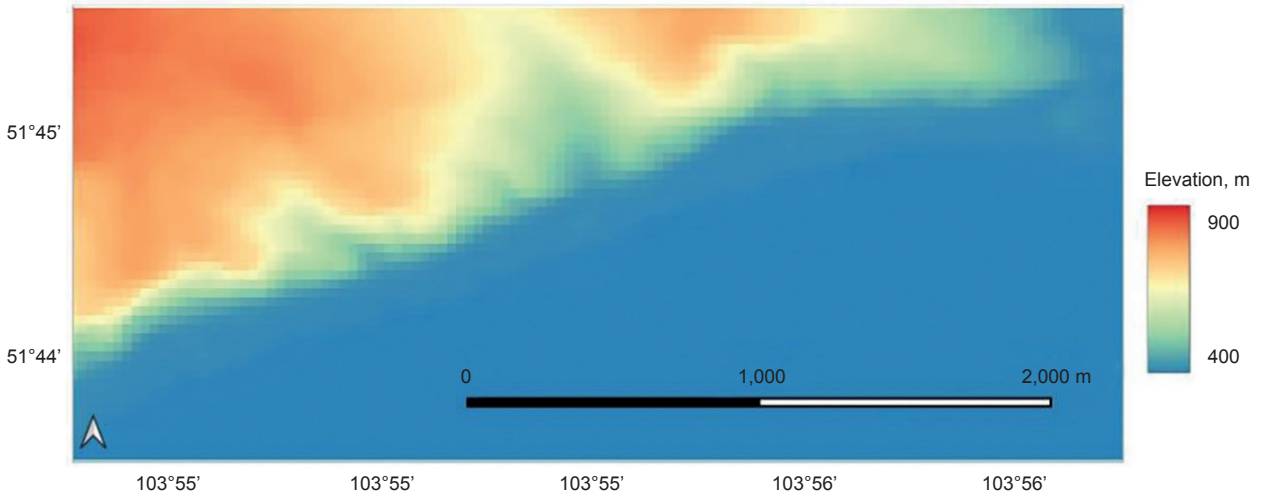

Fig. 1. Digital elevation model of the study area based on AW3D30 data
Рис. 1. Цифровая модель рельефа участка по данным AW3D30

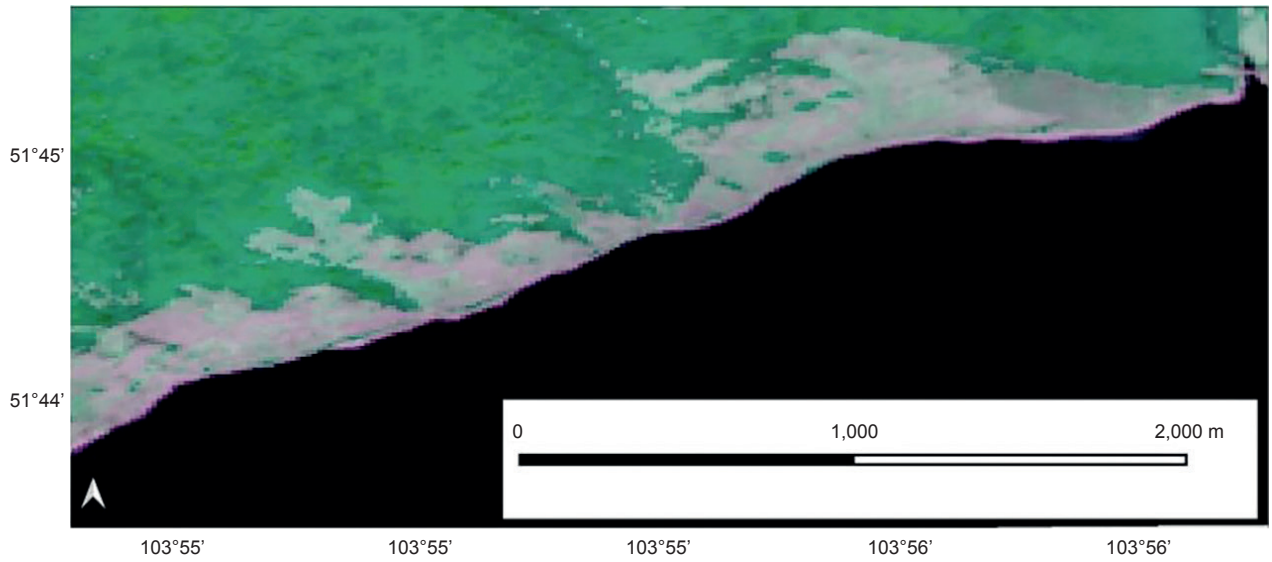

Fig. 2. RGB composite based on Sentinel-2 satellite system data
Рис. 2. RGB-композит по данным спутниковой системы Sentinel-2

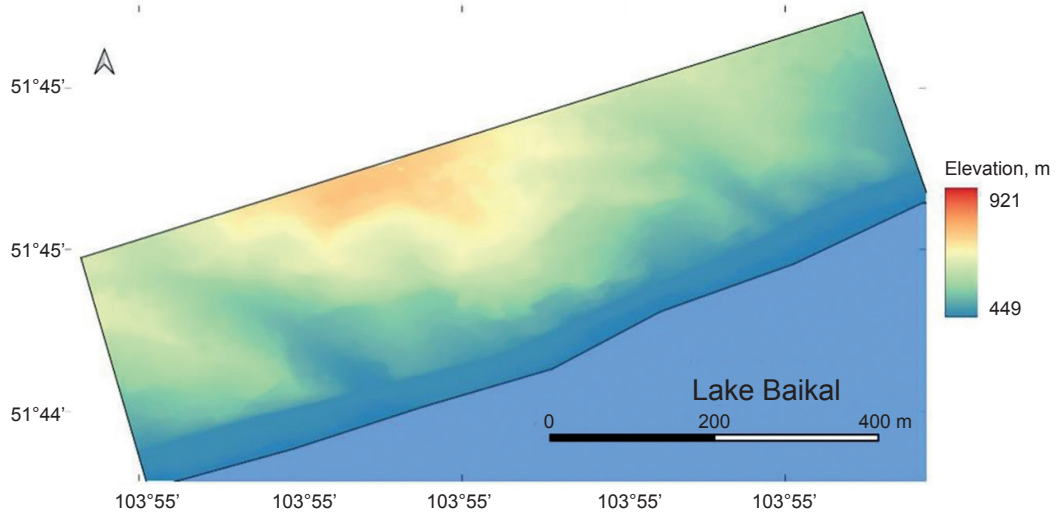

Fig. 3. Digital elevation model derived from unmanned aerial vehicle imagery
Рис. 3. Цифровая модель рельефа по данным съемки с беспилотного летательного аппарата

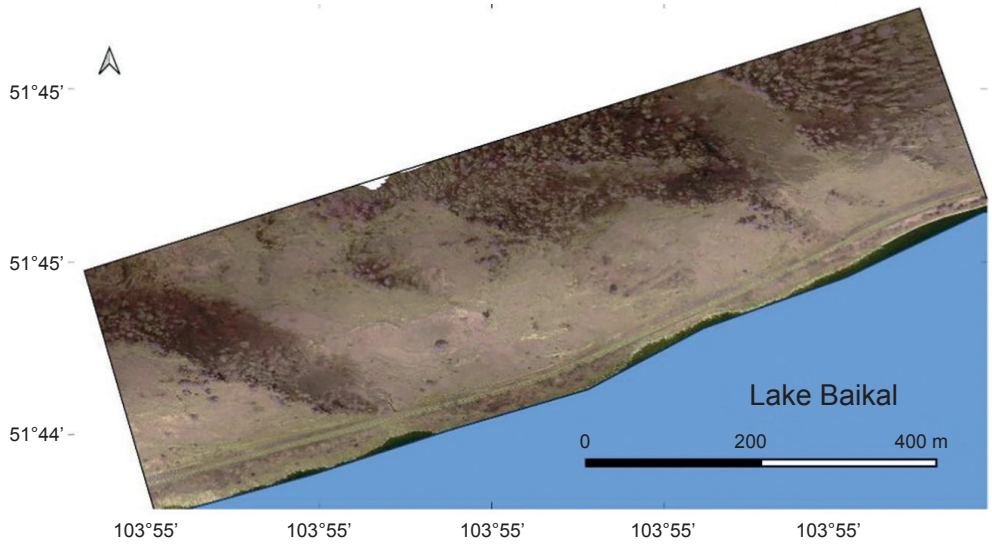

Fig. 4. Orthomosaic (derived from unmanned aerial vehicle imagery)
Рис. 4. Ортофотоплан (по данным съемки с беспилотного летательного аппарата)

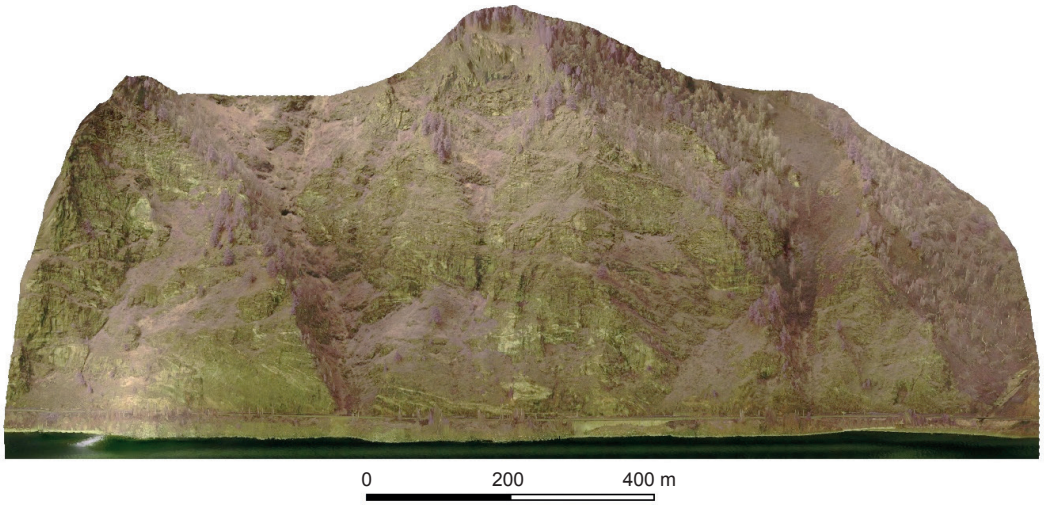

Fig. 5. Front view of the textured site model (derived from unmanned aerial vehicle imagery)
Рис. 5. Вид спереди на текстурированную модель участка работ (по данным съемки с беспилотного летательного аппарата)

landslides is directly related to slope steepness, so slope angle is a key factor in modeling. As the slope angle gets steeper, the gravitational force acting on the rocks also increases, which raises the likelihood of a collapse.

2. Profile curvature is negative for slope increasing downhill (convex flow profile, typical of upper slopes) and positive for slope decreasing downhill (concave, typical of lower slopes). Research indicates that while concave slopes can be areas of lower instability, rockfalls are more common on convex slopes. For convex-shaped slopes, a turning corner usually has negative effects on stability, especially when the corner is relatively small and the thinner exposed slope mass greatly reduced the slope stability [20].

3. LSF (Length-Slope Factor) represents the power of overland flow and the influence of topography on soil erosion risk. It is usually used in soil erosion assessment models (e.g., USLE and RUSLE). The longer and steeper the slope, the higher the velocity and volume of surface runoff, and the more soil is lost [21].

4. WI (Wetness Index) serves as an indicator of soil saturation; the WI is calculated as the natural logarithm of the ratio between the drainage area and the slope. A higher index value correlates with increased soil moisture content. Furthermore, the WI highlights drainage directions that align with preferred paths for landslides [3].

5. NDVI (Normalized Difference Vegetation Index) is a popular vegetation index, that was adopted to identify areas covered by vegetation and bare soil. Land cover factor is significant to consider, as soil strength is enhanced by the presence of roots and the binding of soil layers. Thus, surfaces not covered by vegetation are more susceptible to landslides [22].

Authors used the same AHP models for satellite based and UAV bases data analysis. For determination how much more important one factor is than another pairwise comparison was carried out (Table 1).

The factors involved have different scales and prior to weighed sum calculation, it is essential to normalize the values. To accomplish this, a reclassification was conducted in accordance with Table 2.

The final calculation was carried out in QGIS using the following equation:

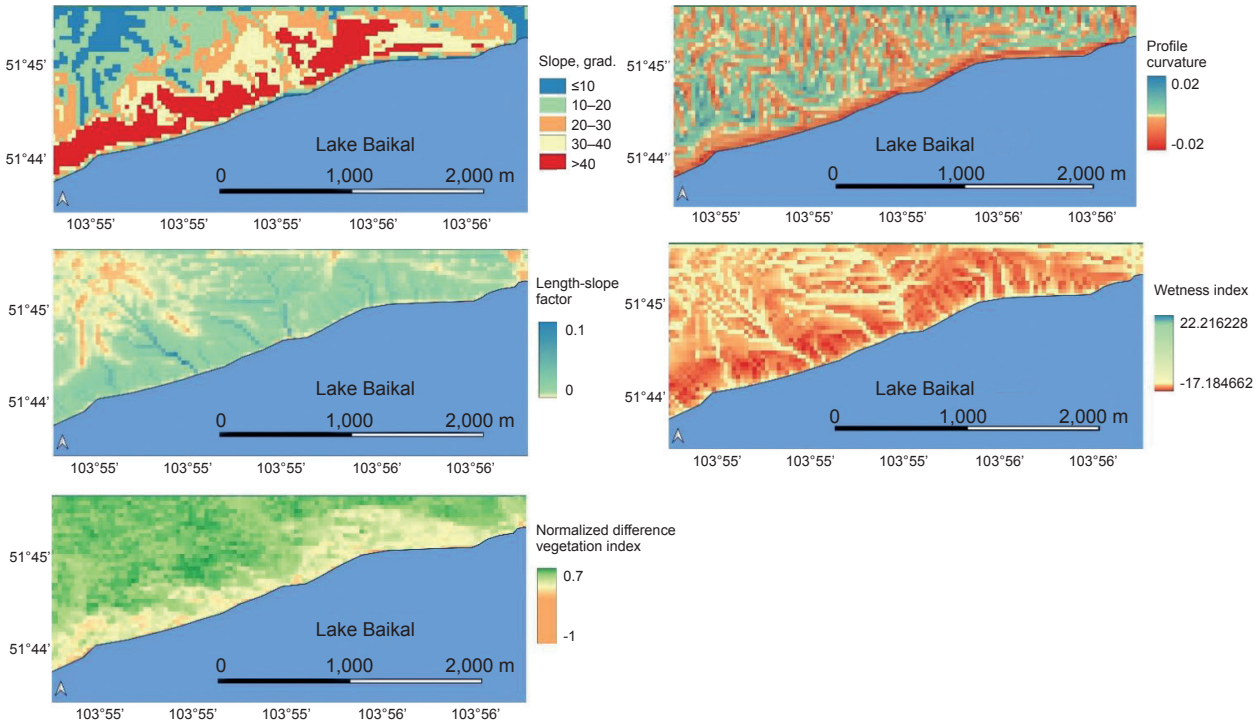

Fig. 6. Satellite-derived maps of environmental factors
Рис. 6. Карты факторов, влияющих на условия окружающей среды, полученные на основе спутниковых данных

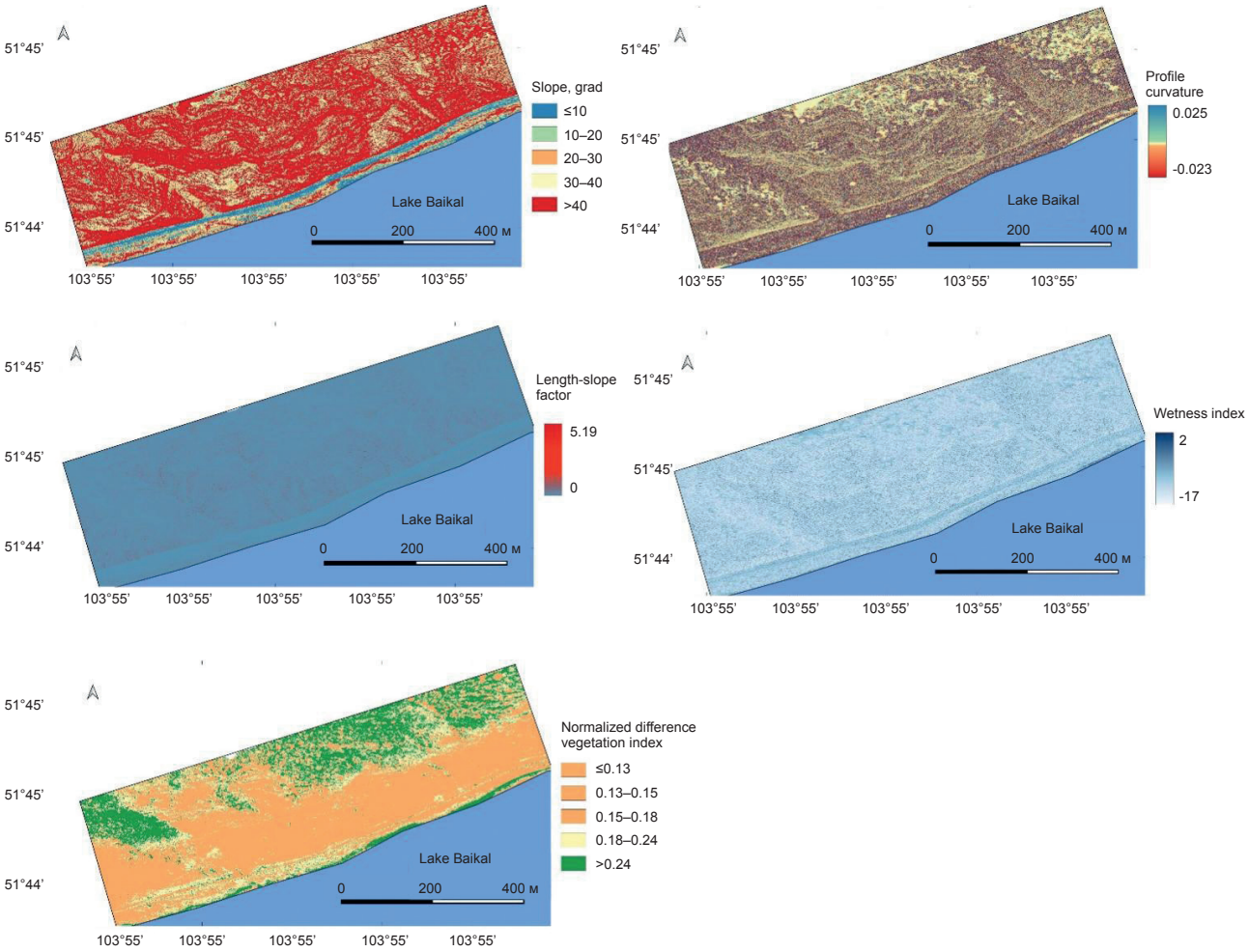

Fig. 7. UAV-derived maps of flight environment factors
Рис. 7. Карты факторов, влияющих на условия полета, полученные на основе данных съемки с беспилотного летательного аппарата

Таблица 1. Матрица попарного сравнения и весовые коэффициенты факторов
Table 1. Pairwise comparison matrix and factor weighting coefficients

Factor	Slope	Normalized difference vegetation index	Wetness index	Profile curvature	Length-slope factor	Weight	Ratio, %
Slope	1.00	3.00	4.00	5.00	6.00	0.48	48
Normalized difference vegetation index	0.33	1.00	2.00	3.00	4.00	0.21	21
Wetness index	0.25	0.50	1.00	2.00	3.00	0.13	13
Profile curvature	0.20	0.33	0.50	1.00	2.00	0.09	9
Length-slope factor	0.17	0.25	0.33	0.50	1.00	0.06	6

$$Susceptibility\ Index = (Slope_{Weight} \times Slope_{Reclass}) + (LSF_{Weight} \times LSF_{Reclass}) + (Curvature_{Weight} \times Curvature_{Reclass}) + (Wetness_{Weight} \times Wetness_{Reclass}) + (NDVI_{Weight} \times NDVI_{Reclass}).$$

Results and discussion

The thematic map of LS spatial distribution was generated and then, it was categorized in five classes (Fig. 8, 9).

Upon visual inspection and superposition of the two final maps, it was revealed that the hazardous zones are spatially located similarly, but the area of the zones differs. Obviously, the reason of this mismatch is different resolution of the DEMs. Spatial resolution limits satellite's ability to detect precise borders of high susceptibility zones. Sharp topographic discontinuities that usually signal unstable slope sections are smoothed out by low-resolution DEMs since they average variables across pixels.

Table 2. Principles of reclassification
Таблица 2. Принципы переклассификации

Factor	Class range	Susceptibility score (1–5)
Slope	0–10° (flat)	1 (low risk)
	10–20°	2
	20–30°	3
	30–40°	4
	>40° (steep)	5 (high risk)
Normalized difference vegetation index	High green (dense forest)	1 (low risk – protection)
	Low/bare soil	5 (high risk)
Wetness index	Low (dry)	1 (low risk)
	High (saturated)	5 (high risk – unstable)
Profile curvature	Convex (diverging flow)	1
	Flat	3
	Concave (converging flow/erosion)	5 (high risk)
Length-slope factor	Low values (low energy)	1
	High values (high energy)	5 (high risk)

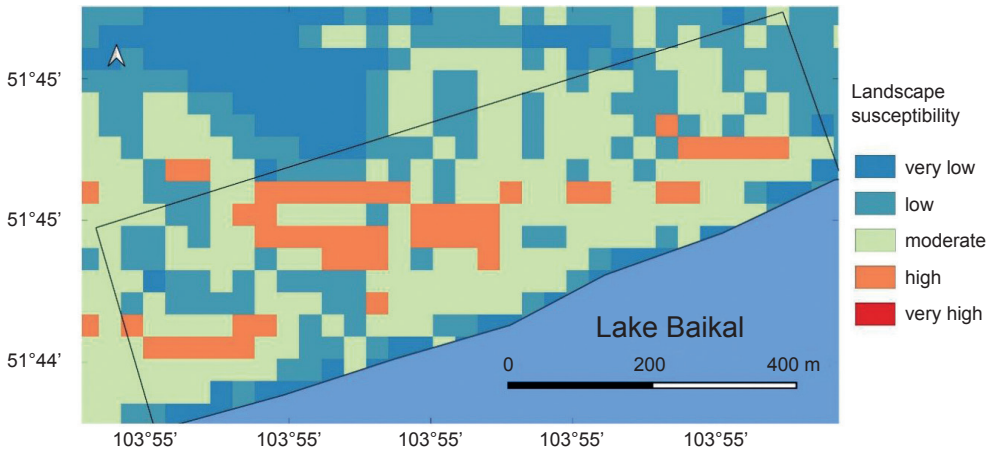

Fig. 8. Satellite-derived landslide susceptibility map
Рис. 8. Карта рисков оползневой опасности на основе спутниковых данных

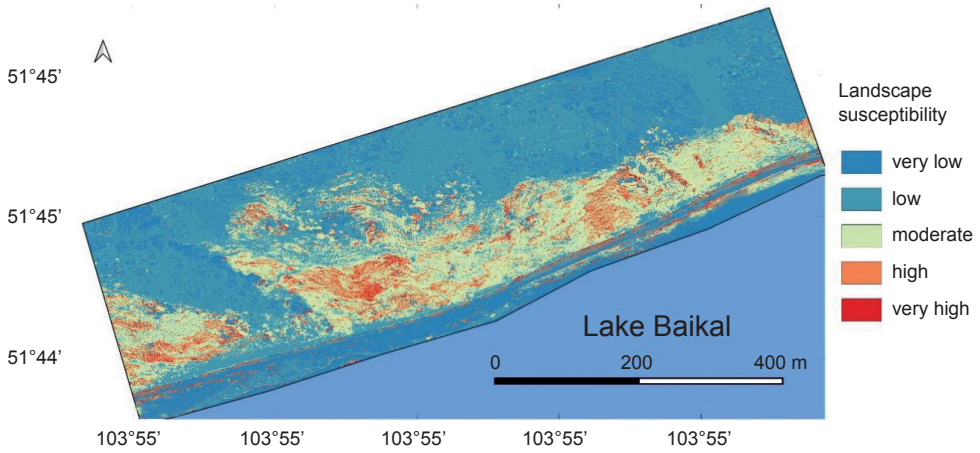

Fig. 9. UAV-derived landslide susceptibility map
Рис. 9. Карта рисков оползневой опасности на основе данных с беспилотного летательного аппарата

A practical takeaway is that 30 m resolution DEM is sufficient for regional LSM, it available to correctly identify unstable slopes that cover the area larger than pixel size. Due to resolution-related generalization, small, unstable rock blocks may increase the vulnerability of the adjacent slope area or, conversely, remain unnoticed.

The practical implications for landslide mitigation measures are significant. A 30-meter-resolution DEM may be sufficient for determining slope instability, but it cannot serve as the basis for engineering design. For example, the effective placement of rock barriers necessitates a detailed understanding of the precise trajectories of falling blocks, which in turn requires a DEM with a resolution of at least 0.5 meters. Similarly, estimating the volume of warning cuts requires precise measurements to avoid unnecessary costs. Acquisition oh high-resolution UAV data is justified when it is required not only determine susceptibility level and spatial extent of at-risk areas, but also provide comprehensive reliable data for mitigation measures design.

One of the advantages of photogrammetry is the ability to create a detailed 3D model of the slope. Viewing the slope not only from the nadir but also from other planes allows one to identify unstable rock blocks, scree, and rock debris at the foot of the slope, indicating past rockfalls. A front view of the slope also allows one to calculate rock fracturing, an important indicator when assessing the instability of a rocky slope [23]. Besides, when rock avalanches potential trajectory is required to be identified, detailed and accurate model of the slope is necessary. Thus, while satellite data serves as a preliminary screening tool, UAV data is essential for any subsequent phase of landslide mitigation design.

Low-resolution satellite data and high-resolution UAV data are not mutually exclusive but rather serve different spatial scales and research questions. Satellite data excel at regional studying and zonation, while UAV data are beneficial for local-scale, detailed mapping.

Conclusion

This study compared low-resolution satellite data (ALOS AW3D30, Sentinel-2) with high-resolution UAV data for LSM in a test area. The key finding is that while both methods identify similar hazardous zones spatially, the area and boundaries of these zones differ substantially due to resolution-related generalization. Specifically, 30 m resolution data overestimate moderate susceptibility zones and miss small hazardous areas that are clearly captured by UAV surveys.

Spatial coverage and obtaining continuous data, particularly in hard-to-reach areas and on dangerous steep slopes, limits traditional field mapping. Remote sensing offers significant advantages over field surveys, including wider coverage and multi-temporal data. Freely available

satellite data enables regional-scale LSM with resolutions up to 10 m. However, low-resolution maps might fail to accurately represent risks in unstable areas. Commercial high-resolution satellite imagery provides necessary detail but is costly due to minimum scene sizes, it is especially noticeable when examining elongated linear objects.

As expected, the resolution of the data influences the outcomes of LSM. Altogether, obtained results support the view that satellite and UAV data are complementary. Hybrid approaches, in which spaceborne data are used for primary zonation and UAV data are employed for precise investigation of hotspots, are therefore recommended.

References

1. Ado M., Amitab K., Maji A.K., Jasińska E., Gono R., Leonowicz Z., et al. Landslide susceptibility mapping using machine learning: a literature survey. *Remote Sensing*. 2022;14(13):3029. https://doi.org/10.3390/rs14133029.

2. Sarkar S., Kanungo D. An integrated approach for landslide susceptibility mapping using remote sensing and GIS. *Photogrammetric Engineering and Remote Sensing*. 2004;70(5):617-625. https://doi.org/10.14358/PERS.70.5.617.

3. Gantimurova S., Parshin A., Erofeev V. GIS-based landslide susceptibility mapping of the Circum-Baikal railway in Russia using UAV data. *Remote Sensing*. 2021;13(18):3629. https://doi.org/10.3390/rs13183629.

4. Casagli N., Frodella W., Morelli S., Tofani V., Ciampalini A., Intrieri E., et al. Spaceborne, UAV and ground-based remote sensing techniques for landslide mapping, monitoring and early warning. *Geoenvironmental Disasters*. 2017;4(1):1-23. https://doi.org/10.1186/s40677-017-0073-1.

5. Rossi G., Tanteri L., Tofani V., Vannocci P., Moretti S., Casagli N. Multitemporal UAV surveys for landslide mapping and characterization. *Landslides*. 2018;15(5):1045-1052. https://doi.org/10.1007/s10346-018-0978-0.

6. Ghorbanzadeh O., Didehban K., Rasouli H., Kamran K.V., Feizizadeh B., Blaschke T. An application of Sentinel-1, Sentinel-2, and GNSS data for landslide susceptibility mapping. *ISPRS International Journal of Geo-Information*. 2020;9(10):561. https://doi.org/10.3390/ijgi9100561.

7. Kyriou A., Nikolakopoulos K. Assessing the suitability of Sentinel-1 data for landslide mapping. *European Journal of Remote Sensing*. 2018;51(1):402-411. https://doi.org/10.1080/22797254.2018.1444944.

8. Lu P., Shi W., Wang Q., Li Z., Qin Y., Fan X. Co-seismic landslide mapping using Sentinel-2 10-m fused NIR narrow, red-edge, and SWIR bands. *Landslides*. 2021;18(6):2017-2037. https://doi.org/10.1007/s10346-021-01636-2.

9. Novellino A., Pennington C., Leeming K., Taylor S., Alvarez I.G., McAllister E., et al. Mapping landslides from space: a review. *Landslides*. 2024;21(5):1041-1052. https://doi.org/10.1007/s10346-024-02215-x.

10. Uuemaa E., Ahi S., Montibeller B., Muru M., Kmoch A. Vertical accuracy of freely available global digital elevation models (ASTER, AW3D30, MERIT, TanDEM-X, SRTM, and NASADEM). *Remote Sensing.* 2020;12(21):3482. https://doi.org/10.3390/rs12213482.

11. González-Moradas M.R., Viveen W., Vidal-Villalobos R.A., Villegas-Lanza J.C. A performance comparison of SRTM v. 3.0, AW3D30, ASTER GDEM3, Copernicus and TanDEM-X for tectonogeomorphic analysis in the South American Andes. *Catena*. 2023;228(3):107160. https://doi.org/10.1016/j.catena.2023.107160.

12. Sun J., Yuan G., Song L., Zhang H. Unmanned aerial vehicles (UAVs) in landslide investigation and monitoring: a review. *Drones*. 2024;8(1):30. https://doi.org/10.3390/drones8010030.

13. Sozzi M., Kayad A., Gobbo S., Cogato A., Sartori L., Marinello F. Economic comparison of satellite, plane and uav-acquired NDVI images for site-specific nitrogen application: observations from Italy. *Agronomy.* 2021;11(11):2098. https://doi.org/10.3390/agronomy11112098.

14. Abramova Z.V., Litvintseva Z.O. Mapping of modern exogenous processes of the central ecological zone of the Baikal natural territory. *The Bulletin of Irkutsk State University. Series: Earth Sciences*. 2023;44:3-17. (In Russ.). https://doi.org/10.26516/2073-3402.2023.44.3.

15. Chandra N., Elizabath, Choudhury S., Vaidya H. Integrated spatial landslide risk assessment for population and infrastructure in Tehri, Garhwal Himalayas, India. *Geological Journal*. 2026. https://doi.org/https://doi.org/10.1002/gj.70251.

16. Das M., Gautam G.K., Jain S., Bhat M.F., Mankar A.K., Koner R. A comparative analysis of AHP, FR, AHP-FR and LR models for landslide susceptibility mapping in Sikkim Himalaya, India. *Earth Surface Processes and Landforms*. 2026;51(2):e70257. https://doi.org/10.1002/esp.70257.

17. Sisay T., Tesfaye G., Jothimani M., Reda T.M., Tadese A. Landslide susceptibility mapping using combined geospatial, FR and AHP models: a case study from Ethiopia's highlands. *Discover Sustainability*. 2024;5(1):474. https://doi.org/10.1007/s43621-024-00730-4.

18. Sutawane S., Mitra S. Landslide susceptibility analysis for Irshalwadi, Maharashtra by using analytical hierarchy process on satellite image. In: *Urbanisation and climate change: strategies for sustainable cities through geospatial technologies: 18th DGSI International conference*. Hyderabad: Osmania University; 2023.

19. Mohd M.H., Azman F.N.U.Z., Jusoh A., Rahman M.A.A. Landslide susceptibility mapping at Lebir and Galas River Basins after extreme flood event using weights of evidence. *Journal of Sustainability Science and Management*. 2019;14(2):103-115.

20. Zhou Y., Qi S.-C., Fan G., Chen M.-L., Zhou J.-W. Topographic effects on three-dimensional slope stability for fluctuating water conditions using numerical analysis. *Water*. 2020;12(2):615. https://doi.org/10.3390/w12020615.

21. Schmidt S., Tresch S., Meusburger K. Modification of the RUSLE slope length and steepness factor (LS-factor) based on rainfall experiments at steep alpine grasslands. *MethodsX*. 2019;6:219-229. https://doi.org/10.1016/j.mex.2019.01.004.

22. Kalsnes B., Capobianco V. Use of vegetation for landslide risk mitigation. *Climate adaptation modelling*. Cham: Springer; 2022, p. 77-85. https://doi.org/10.1007/978-3-030-86211-4_10.

23. Gantimurova S., Parshin A. Combined methodology for rockfall susceptibility mapping using UAV imagery data. *Remote Sensing*. 2024;16(1):177. https://doi.org/10.3390/rs16010177.

Список источников

1. Ado M., Amitab K., Maji A.K., Jasińska E., Gono R., Leonowicz Z., et al. Landslide susceptibility mapping using machine learning: a literature survey // Remote Sensing. 2022. Vol. 14. Iss. 13. P. 3029. https://doi.org/10.3390/rs14133029.

2. Sarkar S., Kanungo D. An integrated approach for landslide susceptibility mapping using remote sensing and GIS // Photogrammetric Engineering and Remote Sensing. 2004. Vol. 70. Iss. 5. P. 617–625. https://doi.org/10.14358/PERS.70.5.617.

3. Gantimurova S., Parshin A., Erofeev V. GIS-based landslide susceptibility mapping of the Circum-Baikal railway in Russia using UAV data // Remote Sensing. 2021. Vol. 13. Iss. 18. C. 3629. https://doi.org/10.3390/rs13183629.

4. Casagli N., Frodella W., Morelli S., Tofani V., Ciampalini A., Intrieri E., et al. Spaceborne, UAV and ground-based remote sensing techniques for landslide mapping, monitoring and early warning // Geoenvironmental Disasters. 2017. Vol. 4. Iss. 1. P. 1–23. https://doi.org/10.1186/s40677-017-0073-1.

5. Rossi G., Tanteri L., Tofani V., Vannocci P., Moretti S., Casagli N. Multitemporal UAV surveys for landslide mapping and characterization // Landslides. 2018. Vol. 15. Iss. 5. P. 1045–1052. https://doi.org/10.1007/s10346-018-0978-0.

6. Ghorbanzadeh O., Didehban K., Rasouli H., Kamran K.V., Feizizadeh B., Blaschke T. An application of Sentinel-1, Sentinel-2, and GNSS data for landslide susceptibility mapping // ISPRS International Journal of Geo-Information. 2020. Vol. 9. Iss. 10. P. 561. https://doi.org/10.3390/ijgi9100561.

7. Kyriou A., Nikolakopoulos K. Assessing the suitability of Sentinel-1 data for landslide mapping // European Journal of Remote Sensing. 2018. Vol. 51. Iss. 1. P. 402–411. https://doi.org/10.1080/22797254.2018.1444944.

8. Lu P., Shi W., Wang Q., Li Z., Qin Y., Fan X. Co-seismic landslide mapping using Sentinel-2 10-m fused NIR narrow, red-edge, and SWIR bands // Landslides. 2021. Vol. 18. Iss. 6. P. 2017–2037. https://doi.org/10.1007/s10346-021-01636-2.

9. Novellino A., Pennington C., Leeming K., Taylor S., Alvarez I.G., McAllister E., et al. Mapping landslides from space: a review // Landslides. 2024. Vol. 21. Iss. 5. P. 1041–1052. https://doi.org/10.1007/s10346-024-02215-x.

10. Uuemaa E., Ahi S., Montibeller B., Muru M., Kmoch A. Vertical accuracy of freely available global digital elevation models (ASTER, AW3D30, MERIT, TanDEM-X, SRTM, and NASADEM) // Remote Sensing. 2020. Vol. 12. Iss. 21. P. 3482. https://doi.org/10.3390/rs12213482.

11. González-Moradas M.R., Viveen W., Vidal-Villalobos R.A., Villegas-Lanza J.C. A performance comparison of SRTM v. 3.0, AW3D30, ASTER GDEM3, Copernicus and TanDEM-X for tectonogeomorphic analysis in the South American Andes // Catena. 2023. Vol. 228. Iss. 3. P. 107160. https://doi.org/10.1016/j.catena.2023.107160.

12. Sun J., Yuan G., Song L., Zhang H. Unmanned aerial vehicles (UAVs) in landslide investigation and monitoring: a review // Drones. 2024. Vol. 8. Iss. 1. P. 30. https://doi.org/10.3390/drones8010030.

13. Sozzi M., Kayad A., Gobbo S., Cogato A., Sartori L., Marinello F. Economic comparison of satellite, plane and UAV-acquired NDVI images for site-specific nitrogen application: observations from Italy // Agronomy. 2021. Vol. 11. Iss. 11. P. 2098. https://doi.org/10.3390/agronomy11112098.

14. Абрамова З.В., Литвинцева З.О. Картографирование современных экзогенных процессов центральной экологической зоны Байкальской природной территории // Известия Иркутского государственного университета. Серия: Науки о Земле. 2023. Т. 44. С. 3–17. https://doi.org/10.26516/2073-3402.2023.44.3.

15. Chandra N., Elizabath, Choudhury S., Vaidya H. Integrated spatial landslide risk assessment for population and infrastructure in Tehri, Garhwal Himalayas, India // Geological Journal. 2026. https://doi.org/https://doi.org/10.1002/gj.70251.

16. Das M., Gautam G.K., Jain S., Bhat M.F., Mankar A.K., Koner R. A comparative analysis of AHP, FR, AHP-FR and LR models for landslide susceptibility mapping in Sikkim Himalaya, India // Earth Surface Processes and Landforms. 2026. Vol. 51. Iss. 2. P. e70257. https://doi.org/10.1002/esp.70257.

17. Sisay T., Tesfaye G., Jothimani M., Reda T.M., Tadese A. Landslide susceptibility mapping using combined geospatial, FR and AHP models: a case study from Ethiopia's highlands // Discover Sustainability. 2024. Vol. 5. Iss. 1. P. 474. https://doi.org/10.1007/s43621-024-00730-4.

18. Sutawane S., Mitra S. Landslide susceptibility analysis for Irshalwadi, Maharashtra by using analytical hierarchy process on satellite image // Urbanisation and climate change: strategies for sustainable cities through geospatial technologies: 18th DGSI International conference. Hyderabad: Osmania University, 2023.

19. Mohd M.H., Azman F.N.U.Z., Jusoh A., Rahman M.A.A. Landslide susceptibility mapping at Lebir and Galas River Basins after extreme flood event using weights of evidence // Journal of Sustainability Science and Management. 2019. Vol. 14. Iss. 2. P. 103–115.

20. Zhou Y., Qi S.-C., Fan G., Chen M.-L., Zhou J.-W. Topographic effects on three-dimensional slope stability for fluctuating water conditions using numerical analysis // Water. 2020. Vol. 12. Iss. 2. P. 615. https://doi.org/10.3390/w12020615.

21. Schmidt S., Tresch S., Meusburger K. Modification of the RUSLE slope length and steepness factor (LS-factor) based on rainfall experiments at steep alpine grasslands // MethodsX. 2019. Vol. 6. P. 219–229. https://doi.org/10.1016/j.mex.2019.01.004.

22. Kalsnes B., Capobianco V. Use of vegetation for landslide risk mitigation // Climate adaptation modelling. Cham: Springer, 2022. P. 77–85. https://doi.org/10.1007/978-3-030-86211-4_10.

23. Gantimurova S., Parshin A. Combined methodology for rockfall susceptibility mapping using UAV imagery data // Remote Sensing. 2024. Vol. 16. Iss. 1. P. 177. https://doi.org/10.3390/rs16010177.

Information about the authors / Информация об авторах

Svetlana A. Gantimurova,
Junior Researcher of the Geoinformatics Department,
Siberian School of Geosciences,
Irkutsk National Research Technical University,
Irkutsk, Russian Federation,
lanagant@geo.istu.edu
https://orcid.org/0009-0005-5978-7869
Гантимурова Светлана Анатольевна,
младший научный сотрудник департамента геоинформатики,
институт «Сибирская школа геонаук»,
Иркутский национальный исследовательский технический университет,
г. Иркутск, Российская Федерация,
lanagant@geo.istu.edu
https://orcid.org/0009-0005-5978-7869

Alexander V. Parshin,
Cand. Sci. (Geol. & Mineral.),
Vice-Rector for Geology, Earth and Environmental Sciences,
Irkutsk National Research Technical University,
Irkutsk, Russian Federation,
Senior Researcher of the Laboratory of Geochemistry of Ore Formation and Geochemical Prospecting Methods,
A.P. Vinogradov Institute of Geochemistry,
Siberian Branch of the Russian Academy of Sciences,
Irkutsk, Russian Federation,
✉ sarhin@geo.istu.edu
https://orcid.org/0000-0003-3733-2140
Паршин Александр Вадимович,
кандидат геолого-минералогических наук,
проректор по геологии, наукам о Земле и окружающей среде,
Иркутский национальный исследовательский технический университет,
г. Иркутск, Российская Федерация,
старший научный сотрудник лаборатории геохимии рудообразования и геохимических методов поисков,
Институт геохимии им. А.П. Виноградова
Сибирского отделения Российской академии наук,
г. Иркутск, Российская Федерация,
✉ sarhin@geo.istu.edu
https://orcid.org/0000-0003-3733-2140

Guanwen Huang,
Professor in Geodesy and Disaster Monitoring,
School of Geological Engineering and Geomatics,
Chang'an University,
Xi'an, China,
guanwen@chd.edu.cn
https://orcid.org/0000-0001-5584-5885
Хуан Гуаньвэнь,
профессор в области геодезии и мониторинга стихийных бедствий,
Школа инженерной геологии и геоматики,
Чанъаньский университет,
г. Сиань, Китай,
guanwen@chd.edu.cn
https://orcid.org/0000-0001-5584-5885

Junyuan Li,
PhD (Hydrogeology),
School of Water and Environment,
Chang'an University,
Xi'an, China,
ljy@@chd.edu.cn
https://orcid.org/0009-0001-1531-2192
Ли Цзюньюань,
доктор наук в области гидрогеологии,
Школа водных ресурсов и окружающей среды,
Чанъаньский университет,
г. Сиань, Китай,
ljy@@chd.edu.cn
https://orcid.org/0009-0001-1531-2192

Ce Jing,
PhD (Geodesy and Disaster Monitoring),
School of Geological Engineering and Geomatics,
Chang'an University,
Xi'an, China,
jingce@chd.edu.cn
https://orcid.org/0000-0002-1796-1962
Цзин Це,
доктор наук в области геодезии и мониторинга стихийных бедствий,
Школа инженерной геологии и геоматики,
Чанъаньский университет,
г. Сиань, Китай,
jingce@chd.edu.cn
https://orcid.org/0000-0002-1796-1962

Vyacheslav T. Zalutskii,
Cand. Sci. (Eng.),
Head of the Laboratory of Digital Geodesy,
Siberian School of Geosciences,
Irkutsk National Research Technical University,
Irkutsk, Russian Federation,
zalutskyvt@istu.edu
https://orcid.org/0000-0002-7318-2429
Залуцкий Вячеслав Трофимович,
кандидат технических наук,
заведующий лабораторией цифровой геодезии,
институт «Сибирская школа геонаук»,
Иркутский национальный исследовательский технический университет,
г. Иркутск, Российская Федерация,
zalutskyvt@istu.edu
https://orcid.org/0000-0002-7318-2429

Contribution of the authors / Вклад авторов

Svetlana A. Gantimurova – investigation, visualization, writing – original draft.
Alexander V. Parshin – conceptualization, methodology, writing – original draft, writing – editing.
Guanwen Huang – methodology, investigation, writing – original draft.
Junyuan Li – investigation, writing – original draft.
Ce Jing – investigation, writing – original draft.
Vyacheslav T. Zalutskii – data curation, validation.
С.А. Гантимурова – проведение исследования, визуализация, написание черновика рукописи.
А.В. Паршин – разработка концепции, разработка методологии, написание черновика рукописи, редактирование рукописи.
Г. Хуан – разработка методологии, проведение исследования, написание черновика рукописи.
Ц. Ли – проведение исследования, написание черновика рукописи.
Ц. Цзин – проведение исследования, написание черновика рукописи.
В.Т. Залуцкий – курирование данных, валидация результатов.

Conflict of interests / Конфликт интересов

Alexander V. Parshin has been a member of the editorial board of the Earth Sciences and Subsoil Use journal since 2023, but he did not take part in making decision about publishing the article under consideration. The article was peer reviewed following the journal's review procedure. The authors do not report any other conflicts of interests.

А.В. Паршин является членом редакционной коллегии журнала «Науки о Земле и недропользование» с 2023 года, но не имеет отношения к решению опубликовать эту статью. Статья прошла принятую в журнале процедуру рецензирования. Об иных конфликтах авторы не заявляли.

The final manuscript has been read and approved by all the co-authors.
Все авторы прочитали и одобрили окончательный вариант рукописи.

Information about the article / Информация о статье

The article was submitted 04.02.2026; approved after reviewing 17.02.2026; accepted for publication 25.02.2026.
Статья поступила в редакцию 04.02.2026; одобрена после рецензирования 17.02.2026; принята к публикации 25.02.2026.